ELSEVIER

Comput. Methods Appl. Mech. Engrg. 187 (2000) 245–260

Computer methods in applied mechanics and engineering

www.elsevier.com/locate/cma

Generating conjugate shapes using piecewise cubic spline functions

Shyh-Haur Su, Ching-Huan Tseng *

Department of Mechanical Engineering, National Chiao Tung University, 1001 Ta Hseuh Road, Hsinchu, Hsinchu 30050, Taiwan, ROC

Received 8 June 1998

Abstract

This paper proposes a method called "piecewise generation" for generating conjugate shapes from sets of data points on original cutters using cubic spline functions to fit the points. The differences between conventional generation methods and piecewise generation are presented. The main advantage of this method is that the analytical form of the cutter need not be provided. Therefore, only sets of data points on the cutter either derived from analytical form or measured with coordinate measuring machines (CMMs) are necessary for the conjugate shape to be derived using this method. It provides a practical and useful tool for conjugate-pair design verification and reverse engineering applications. © 2000 Elsevier Science S.A. All rights reserved.

1. Introduction

Mechanisms are said to have conjugate shapes if they transform motions using prescribed functions [1–3]. Conjugate kinematic pairs are important transmission mechanisms used in gearing pairs, cams and followers, or screw compressor rotors, etc. However, most conjugate machine parts are designed using elementary geometric figures such as points, straight lines, involute curves, arcs and curves combined in appropriate ways. Simple shapes are always chosen as long as more complicated shapes are not required for production reasons [4]. Whereas, when produced profiles greatly influence performance, and more complicated shapes are required for functional reasons, changes in shape parameters always entail geometric constraints, including those on properties of curves, and those on the mathematical continuities of adjacent curves and their points of tangency [5–7].

Cubic spline is one of the geometric curve descriptions with first- and second-derivative continuities. It gives a curve-fitting solution as an approximate model. However, many papers have discussed various numerical methods about curve fitting to reduce the fitting errors. Furthermore, for reverse engineering applications, the digitized data may be coupled with the machining error and system error of the used measuring machine. Though the measured data can be exactly fitted, the use of interpolation in the data may result in unexpected oscillations on the derivatives. Wagner et al. [8] used spring spline for smoothing curvature and torsion, and its piecewise parametric cubic spline functions can avoid the spurious oscillations in derivatives.

Most commonly used method for generating conjugate shapes is a conventional one that employs cutters identical in analytical form (or parametric form) to product geometric shapes. Only after the analytical form of the cutter is determined can the meshing equation and the coordinate-transformation equations be

* Corresponding author. Tel.: +886-3-5726111 Ext. 55129; fax: +886-3-5717243.
E-mail address: chtseng@cc.nctu.edu.tw (C.-H. Tseng).

0045-7825/00/$ - see front matter
PII: S0045-7825(99)00133-4

derived and solved simultaneously to obtain the conjugate shapes. If a cutter shape is changed, the equation of meshing has to be derived again, which requires additional time to do routine procedures. Conventional generation methods also cannot implement discrete data points on the cutters because meshing equations cannot be derived from these discrete points.

This paper proposes a generation method based on numerical considerations. The cutters are simulated using piecewise curves by dividing the original cutter into many small sections, and are treated as sets of small cutters. It can apply gearing theory to generate conjugate shapes using these small cutters, and compare the work-piece errors produced by the original cutter with those produced by the curve-fitted ones. This method is called "piecewise generation". Su and Tseng [9] discussed a variation of this method that uses piecewise linear functions to fit the data points, but the existence of tip points among the piecewise linear cutters leads to point generation, making the linear function approach seem not very suitable for practical applications. The choices number of data point and its fitting methods have a significant influence on the resulting generated conjugate shapes. In this paper, the cubic spline method was chosen and all data points either derived from the analytical form or measured with CMMs are used for curve fitting.

2. Conventional generation method

In order to explain the difference between the conventional generation method and the piecewise generation method, two fundamental examples are introduced in the present study to show procedures for solving problems using these methods.

Case 1: Rack cutter generating involute teeth.

Consider the coordinate systems shown in Fig. 1. The shape of the rack tooth is represented in coordinate system S_1 by the equations

$$\mathbf{r}_1(\theta) = \theta \sin\psi_c \mathbf{i}_1 + \theta \cos\psi_c \mathbf{j}_1, \tag{1}$$

$$-\theta_1 < \theta < \theta_2, \tag{2}$$

$$O_1M = \theta. \tag{3}$$

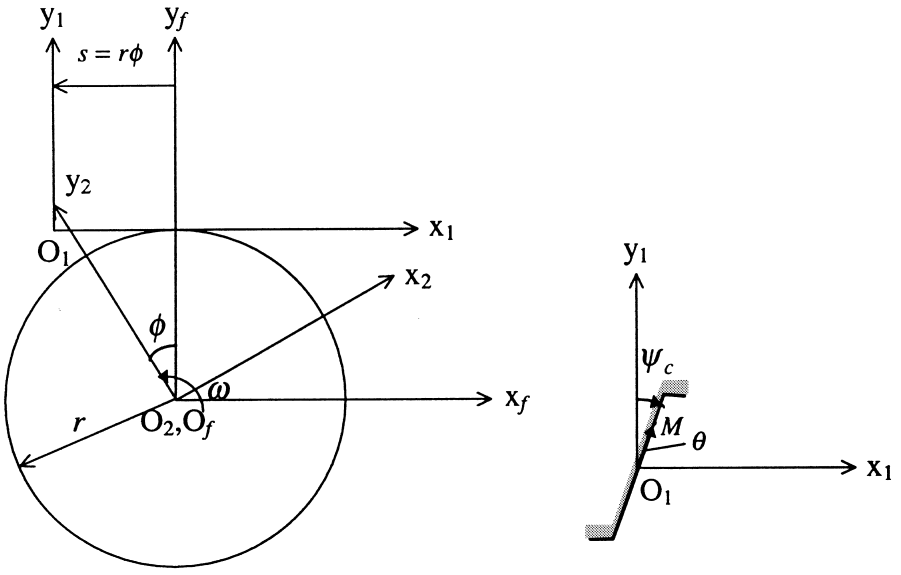

Fig. 1. Generation mechanism for case 1.

Table 1
Parameter values in case 1 used for the conventional generation method

Parameters	Values
r	7.2 mm
ψ_c	20°
θ	$-1 \leqslant \theta \leqslant 1$
n	5

The rack displacement and the angle of gear rotation ϕ are related by

$$\frac{s}{\phi} = r \quad (r \text{ is constant}). \tag{4}$$

The values of the shape parameters are shown in Table 1. Find the conjugate shape generated by the rack cutter.

Solution

Equation of meshing: Using the equation of meshing

$$\mathbf{N}_1 \cdot \mathbf{v}_1^{(12)} = 0, \tag{5}$$

it can be got (see Appendix A)

$$f_1(\theta, \phi) = \theta - r\phi \ \sin\psi_c = 0. \tag{6}$$

Conjugate shape Σ_2: The shape Σ_1 represented in coordinate system S_2 is

$$\begin{aligned}[\mathbf{r}_2] &= [\mathbf{M}_{21}][\mathbf{r}_1] = [\mathbf{M}_{2f}][\mathbf{M}_{f1}][\mathbf{r}_1] \\ &= \begin{bmatrix} \cos\phi & \sin\phi & 0 \\ -\sin\phi & \cos\phi & 0 \\ 0 & 0 & 1 \end{bmatrix} \begin{bmatrix} 1 & 0 & -s \\ 0 & 1 & r \\ 0 & 0 & 1 \end{bmatrix} \begin{bmatrix} \theta\sin\psi_c \\ \theta\cos\psi_c \\ 1 \end{bmatrix} \\ &= \begin{bmatrix} -r\phi\cos\phi + r\sin\phi + \theta\sin(\phi+\psi_c) \\ r\phi\sin\phi + r\cos\phi + \theta\cos(\phi+\psi_c) \\ 1 \end{bmatrix}. \end{aligned} \tag{7}$$

Then, the equations for shape Σ_2 are

$$x_2 = -r\phi\cos\phi + r\sin\phi + \theta\sin(\phi+\psi_c), \tag{8}$$

$$y_2 = r\phi\sin\phi + r\cos\phi + \theta\cos(\phi+\psi_c), \tag{9}$$

$$\theta - r\phi\sin\psi_c = 0 \tag{10}$$

and the shape is as plotted in Fig. 2.

Case 2: Involute pinion generating an involute gear.

Consider the coordinate systems shown in Fig. 3. The shape of the involute tooth is represented in coordinate system S_2 by the equations

$$x_1 = r_b(\sin\theta - \theta\cos\theta), \tag{11}$$

$$y_1 = r_b(\cos\theta + \theta\sin\theta), \tag{12}$$

$$-\theta_1 < \theta < \theta_2, \tag{13}$$

where r_b is the radius of the base circle. The shape parameter values are shown in Table 2. Find the conjugate shape generated by the involute teeth of the pinion.

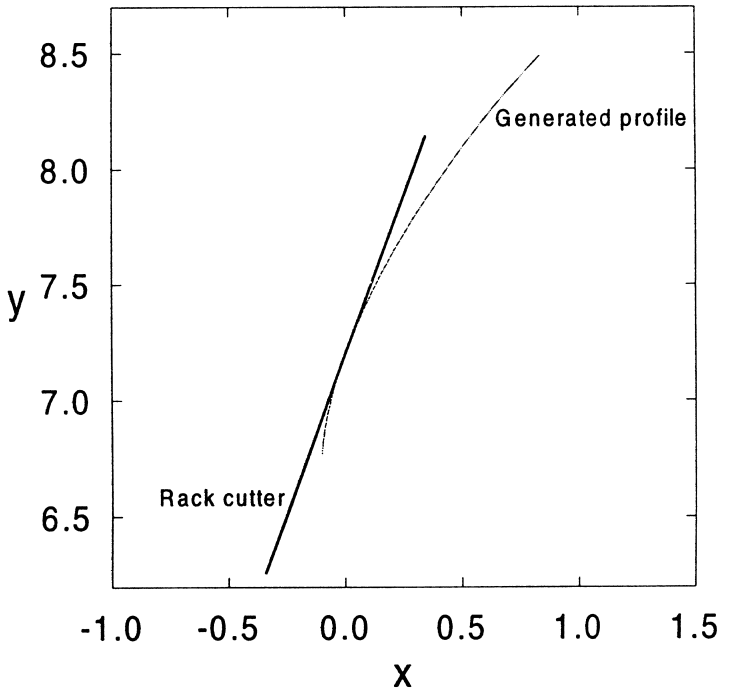

Fig. 2. Theoretical conjugate shape for case 1.

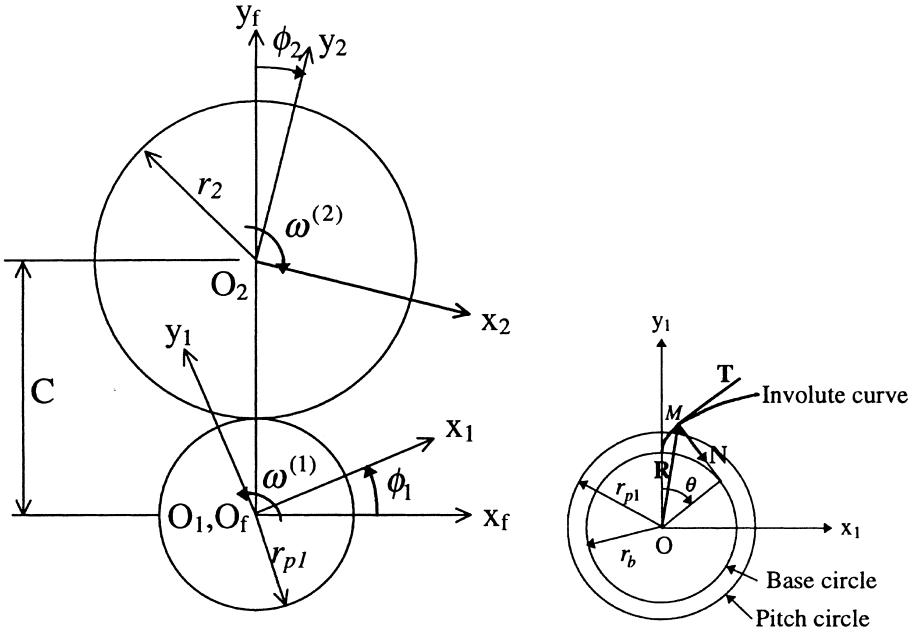

Fig. 3. Generation mechanism for case 2.

Solution

Equation of meshing: The equation of meshing is

$$\mathbf{N}_1 \cdot \mathbf{v}_1^{(12)} = 0 \tag{14}$$

and that yields (see Appendix B)

Table 2
Parameter values in case 2 used for the conventional generation method

Parameters	Values
r_b	6.766 (mm)
r_{p1}	7.2 (mm)
r_{p2}	18 (mm)
N_1	16 (teeth)
N_2	40 (teeth)
θ	$0^\circ \leqslant \theta \leqslant 50^\circ$
n	5

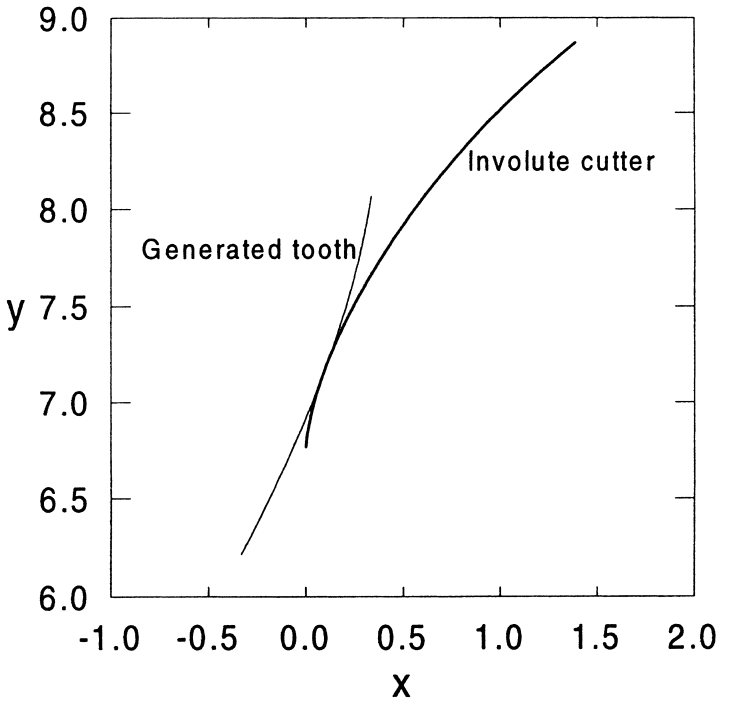

Fig. 4. Involute theoretical results for case 2.

$$f_2(\theta,\phi_1)=\cos\theta\left[-y_1\left(\frac{m_{12}+1}{m_{12}}\right)-\frac{C\cos\phi_1}{m_{12}}\right]-\sin\theta\left[x_1\left(\frac{m_{12}+1}{m_{12}}\right)-\frac{C\sin\phi_1}{m_{12}}\right]=0. \tag{15}$$

Conjugate shape Σ_2: The shape Σ_1 represented in coordinate system S_2 is

$$\begin{aligned}[\mathbf{r}_2]&=[\mathbf{M}_{21}][\mathbf{r}_1]=[\mathbf{M}_{2f}][\mathbf{M}_{f1}][\mathbf{r}_1]\\&=\begin{bmatrix}\cos\phi_2 & -\sin\phi_2 & C\sin\phi_2\\ \sin\phi_2 & \cos\phi_2 & -C\cos\phi_2\\ 0 & 0 & 1\end{bmatrix}\begin{bmatrix}\cos\phi_1 & -\sin\phi_1 & 0\\ \sin\phi_1 & \cos\phi_1 & 0\\ 0 & 0 & 1\end{bmatrix}\begin{bmatrix}r_b(\sin\theta-\theta\cos\theta)\\ r_b(\cos\theta+\theta\sin\theta)\\ 1\end{bmatrix}\\&=\begin{bmatrix}C\sin\phi_2+r_b[-\sin(\phi_1+\phi_2)(\cos\theta+\theta\sin\theta)+\cos(\phi_1+\phi_2)(\sin\theta-\theta\cos\theta)]\\ -C\cos\phi_2+r_b[\sin(\phi_1+\phi_2)(\sin\theta-\theta\cos\theta)+\cos(\phi_1+\phi_2)(\cos\theta+\theta\sin\theta)]\\ 1\end{bmatrix}.\end{aligned} \tag{16}$$

The equations for shape Σ_2 are

$$x_2 = C\sin\phi_2 + r_b[-\sin(\phi_1+\phi_2)(\cos\theta+\theta\sin\theta)+\cos(\phi_1+\phi_2)(\sin\theta-\theta\cos\theta)], \tag{17}$$

$$y_2 = -C\cos\phi_2 + r_b[\sin(\phi_1+\phi_2)(\sin\theta-\theta\cos\theta)+\cos(\phi_1+\phi_2)(\cos\theta+\theta\sin\theta)], \tag{18}$$

$$f_2(\theta,\phi_1) = 0 \tag{19}$$

and the shape is as plotted in Fig. 4.

3. Piecewise generation method

3.1. Cubic spline interpolation

Consider the cases in the preceding section, but with only discrete points on the cutter being given. Cubic spline functions are used to connect the discrete points located on the original cutter, after which they can be treated as a set of small cutters, no matter what type of original cutter is considered.

Assume that the data point coordinates are

$$\{(x_i,y_i)|i=1,2,\ldots,n+1\}, \tag{20}$$

where n means the total number of piecewise cubic spline curves. The parametric form of cubic spline functions that pass through these data points in coordinate system S_1 can then be represented as

$$\mathbf{r}_i = [X_i(u)\ Y_i(u)], \quad i=1,2,\ldots,n, \tag{21}$$

where

$$X_i(u) = a_i + b_iu + c_iu^2 + d_iu^3, \tag{22}$$

$$Y_i(u) = e_i + f_iu + g_iu^2 + h_iu^3, \tag{23}$$

$$0 \leqslant u \leqslant 1. \tag{24}$$

In general, the x-coordinates $X(u)$ of points on a curve are determined solely by the x-coordinates $x_0,\ldots,x_{n+1}$ of the data points, and similarly $Y(u)$ coordinates are determined solely by the y-coordinates of the data points. Each $X_i(u)$ is a cubic polynomial in the parameter u. Their coefficients $a_i,b_i,\ldots,h_i$ can be determined by *Hermite interpolation*, and can be generalized to higher-order polynomials [7].

Notice that the *natural cubic spline* is chosen here, that is, the second-order derivatives at the endpoints are both required being zero

$$X_1^{(2)}(0) = 0, \quad X_{n+1}^{(2)}(1) = 0, \tag{25}$$

$$Y_1^{(2)}(0) = 0, \quad Y_{n+1}^{(2)}(1) = 0. \tag{26}$$

Since the parametric form of $\mathbf{r}_i$ has been determined, its tangent

$$\begin{aligned}\mathbf{T}_{i1} &= \frac{\partial \mathbf{r}_i}{\partial u}\\ &= (b_i+2c_iu+3d_iu^2)\mathbf{i}_1 + (f_i+2g_iu+3h_iu^2)\mathbf{j}_1\\ &\equiv x_{ti}(u)\mathbf{i}_1 + y_{ti}(u)\mathbf{j}_1\end{aligned} \tag{27}$$

and its normal

$$\begin{aligned}\mathbf{N}_{i1} &= \frac{\mathrm{d}\mathbf{r}_i}{\mathrm{d}u}\times\mathbf{k}_1\\ &= (f_i+2g_iu+3h_iu^2)\mathbf{i}_1 - (b_i+2c_iu+3d_iu^2)\mathbf{j}_1\\ &= y_{ti}(u)\mathbf{i}_1 - x_{ti}(u)\mathbf{j}_1\end{aligned} \tag{28}$$

can also be derived ($i = 1, 2, \ldots, n$). These information will be used for determining the corresponding conjugate shapes.

3.2. Procedures of piecewise generation method

Piecewise generation method can be achieved by the following steps:

Step 1: Data point sampling.

Data points can be got either by evaluating theoretical curves or the measuring results from coordinate measuring machines. Suitable sampling of data points will improve the accuracy of the curve-fitting results. Data points evaluated from theoretical curves for both examples mentioned in previous section are listed in Table 3.

Step 2: Curve fitting.

Various curve-fitting methods can be applied to fit the data points obtained from step 1. If the data points contain machining error or system error of the used measuring machine, it is suitable to apply approaches in the form of least squares to approximated measured points. The spring spline [8] can be applied to avoid the spurious oscillation in derivatives. Su and Tseng [9] used linear functions to fit the data points. However, the piecewise cubic spline function is used in this study since the data points are evaluated from the theoretical curves in the previous two examples.

Step 3: Applying generation method.

The problems given above are solved using the piecewise generation method as follows:

Case 1: Rack cutter generating involute teeth. The number of piecewise cubic spline functions is set at 5, that is to say, $n = 5$.

Relative velocity $\mathbf{v}_i^{(12)}$: As shown in Fig. 1, the velocity of the rack cutter is

$$\mathbf{v}_i^{(1)} = -\omega r \mathbf{i}_1, \tag{29}$$

where ω is the angular velocity of the gear, and r the radius of the pitch circle.

The linear velocity of the gear contact point is

$$\begin{aligned}\mathbf{v}_i^{(2)} &= (\omega \times \mathbf{r}_i) + (\overline{O_1O_2} \times \omega) \\ &= \begin{bmatrix} \mathbf{i}_1 & \mathbf{j}_1 & \mathbf{k}_1 \\ 0 & 0 & \omega \\ X_i(u) & Y_i(u) & 0 \end{bmatrix} + \begin{bmatrix} \mathbf{i}_1 & \mathbf{j}_1 & \mathbf{k}_1 \\ r\phi_i & -r & 0 \\ 0 & 0 & \omega \end{bmatrix} \\ &= \omega[-(Y_i(u) + r)\mathbf{i}_1 + (X_i(u) - r\phi_i)\mathbf{j}_1]. \end{aligned} \tag{30}$$

The relative linear velocity is

$$\mathbf{v}_i^{(12)} = \mathbf{v}_i^{(1)} - \mathbf{v}_i^{(2)} = \omega[Y_i(u)\mathbf{i}_1 + (-X_i(u) + r\phi_i)\mathbf{j}_1]. \tag{31}$$

Equation of meshing. Using the equation of meshing

$$\mathbf{N}_{i1} \cdot \mathbf{v}_i^{(12)} = 0, \tag{32}$$

we get

$$f_{3i}(X_i, \phi) = x_{ti}(u)X_i(u) + y_{ti}(u)Y_i(u) - r\phi_i x_{ti}(u) = 0. \tag{33}$$

Table 3
The sampling data points for case 1 and case 2

	No.	1	2	3	4	5	6
Case 1	x	−0.342	−0.205	−0.068	0.068	0.205	0.342
	y	6.260	6.636	7.012	7.388	7.764	8.139
Case 2	x	0.000	0.012	0.095	0.315	0.731	1.388
	y	6.766	6.868	7.166	7.631	8.219	8.872

Conjugate shape Σ_2: The shape Σ_1 represented in coordinate system S_2 is

$$[\mathbf{r}_{2i}] = [\mathbf{M}_{21}][\mathbf{r}_i] = [\mathbf{M}_{2f}][\mathbf{M}_{f1}][\mathbf{r}_i]$$
$$= \begin{bmatrix} \cos\phi_i & \sin\phi_i & 0 \\ -\sin\phi_i & \cos\phi_i & 0 \\ 0 & 0 & 1 \end{bmatrix} \begin{bmatrix} 1 & 0 & -s \\ 0 & 1 & r \\ 0 & 0 & 1 \end{bmatrix} \begin{bmatrix} X_i(u) \\ Y_i(u) \\ 1 \end{bmatrix}$$
$$= \begin{bmatrix} X_i(u)\cos\phi_i + Y_i(u)\sin\phi_i + r(\sin\phi_i - \phi_i\cos\phi_i) \\ -X_i(u)\sin\phi_i + Y_i(u)\cos\phi_i + r(\phi_i\sin\phi_i + \cos\phi_i) \\ 1 \end{bmatrix}. \tag{34}$$

The equations for shape Σ_2 are:

$$x_2 = X_i(u)\cos\phi_i + Y_i(u)\sin\phi_i + r(\sin\phi_i - \phi_i\cos\phi_i), \tag{35}$$

$$y_2 = -X_i(u)\sin\phi_i + Y_i(u)\cos\phi_i + r(\phi_i\sin\phi_i + \cos\phi_i), \tag{36}$$

$$x_{ti}(u)X_i(u) + y_{ti}(u)Y_i(u) - r\phi_i x_{ti}(u) = 0, \tag{37}$$

where

$$\phi_{\text{lower},i} \leqslant \phi_i \leqslant \phi_{\text{upper},i}, \tag{38}$$

and the generated shape is as plotted in Fig. 5.

In fact, the cubic spline fitting result for the straight line is identical with the original one, and there will not exist errors between generated curves derived from conventional generation and piecewise generation.

Case 2: Consider an involute cutter generating tooth, as shown in Fig. 3.

Relative velocity $\mathbf{v}_1^{(12)}$: From Eqs. (B.3) and (B.4), the ratio of angular velocity changes can be represented by

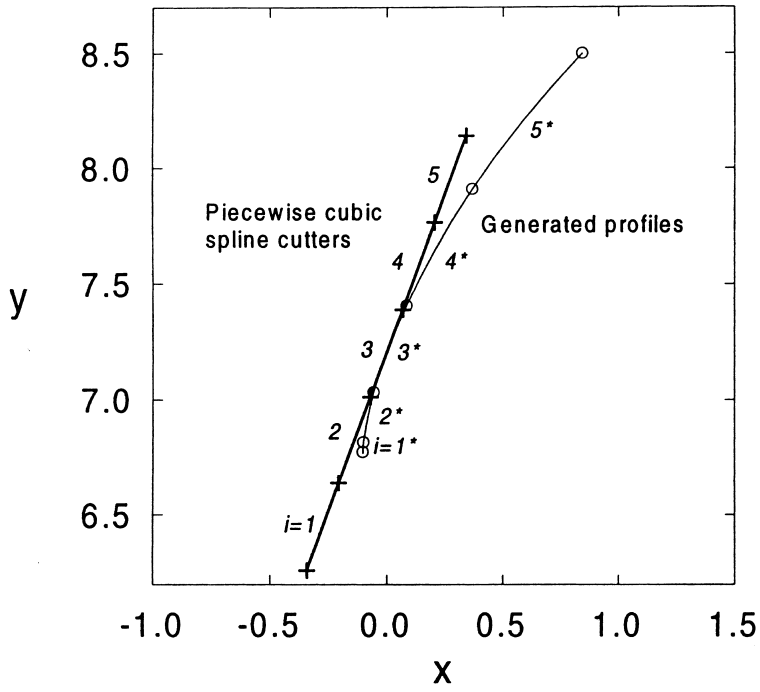

Fig. 5. Piecewise generation results for case 1.

$$m_{12} = \frac{\omega^{(1)}}{\omega^{(2)}} = \frac{\phi_{1i}}{\phi_{2i}} = \frac{N_2}{N_1} \quad (i = 1, 2, \ldots, n), \tag{39}$$

where N_1 and N_2 are respectively, pinion 1 and gear 2 tooth numbers.

The relative linear velocity is

$$\begin{aligned}
\mathbf{v}_i^{(12)} &= \mathbf{v}_i^{(1)} - \mathbf{v}_i^{(2)} = (\omega_1^{(12)} \times \mathbf{r}_i) - (\overline{O_1O_2} \times \omega_1^{(2)}) \\
&= \begin{vmatrix} \mathbf{i}_1 & \mathbf{j}_1 & \mathbf{k}_1 \\ 0 & 0 & \omega_1^{(1)} + \omega_1^{(2)} \\ X_i(u) & Y_i(u) & 0 \end{vmatrix} - \begin{vmatrix} \mathbf{i}_1 & \mathbf{j}_1 & \mathbf{k}_1 \\ C\sin\phi_{1i} & C\cos\phi_{1i} & 0 \\ 0 & 0 & -\omega_1^{(2)} \end{vmatrix} \\
&= -[(\omega_1^{(1)} + \omega_1^{(2)})Y_i(u) - \omega_1^{(2)} C\cos\phi_{1i}]\mathbf{i}_1 + [(\omega_1^{(1)} + \omega_1^{(2)})X_i(u) - \omega_1^{(2)} C\sin\phi_{1i}]\mathbf{j}_1.
\end{aligned} \tag{40}$$

Equation of meshing. The equation of meshing is thus

$$f_{4i}(X_i(u), \phi_{1i}) = \mathbf{N}_i \cdot \mathbf{v}_i^{(12)} = 0. \tag{41}$$

Conjugate shape Σ_2. The shape Σ_1 represented in coordinate system S_2 is

$$\begin{aligned}
[\mathbf{r}_{2i}] &= [\mathbf{M}_{21}][\mathbf{r}_i] = [\mathbf{M}_{2f}][\mathbf{M}_{f1}][\mathbf{r}_i] \\
&= \begin{bmatrix} \cos\phi_{2i} & -\sin\phi_{2i} & C\sin\phi_{2i} \\ \sin\phi_{2i} & \cos\phi_{2i} & -C\cos\phi_{2i} \\ 0 & 0 & 1 \end{bmatrix} \begin{bmatrix} \cos\phi_{1i} & -\sin\phi_{1i} & 0 \\ \sin\phi_{1i} & \cos\phi_{1i} & 0 \\ 0 & 0 & 1 \end{bmatrix} \begin{bmatrix} X_i(u) \\ Y_i(u) \\ 1 \end{bmatrix} \\
&= \begin{bmatrix} C\sin\phi_{2i} - Y_i(u) \cdot \sin(\phi_{1i} + \phi_{2i}) + X_i(u) \cdot \cos(\phi_{1i} + \phi_{2i}) \\ -C\cos\phi_{2i} + X_i(u) \cdot \sin(\phi_{1i} + \phi_{2i}) + Y_i(u) \cdot \cos(\phi_{1i} + \phi_{2i}) \\ 1 \end{bmatrix}.
\end{aligned} \tag{42}$$

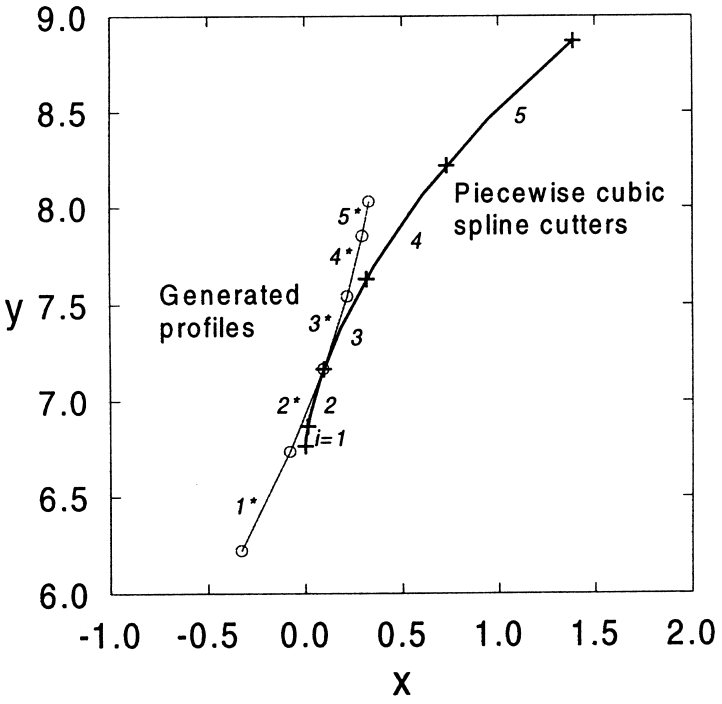

Fig. 6. Piecewise generation results for case 2.

The equations for shape Σ_2 are:

$$x_2 = C\sin\phi_{2i} - Y_i(u)\cdot\sin(\phi_{1i}+\phi_{2i}) + X_i(u)\cdot\cos(\phi_{1i}+\phi_{2i}), \tag{43}$$

$$y_2 = -C\cos\phi_{2i} + X_i(u)\cdot\sin(\phi_{1i}+\phi_{2i}) + Y_i(u)\cdot\cos(\phi_{1i}+\phi_{2i}), \tag{44}$$

$$f_{4i}(X_i(u),\phi_{1i}) = 0, \quad f_{4i}(X_i(u),\phi_{1i}) = \mathbf{N}_i\cdot\mathbf{v}_i^{(12)} = 0. \tag{45}$$

where

$$\phi_{\text{lower},i} \leqslant \phi_{1i} \leqslant \phi_{\text{upper},i}, \tag{46}$$

and the shape is as plotted in Fig. 6.

4. Working ranges of kinematic parameters $\phi_i's$

Since the original cutter has been divided into small piecewise cutters, the determination of kinematic parameters ϕ_i working ranges is very important for every small cubic spline cutter, where ϕ_i is the working range of the ith cutter that does the actual generation.

The limiting values $(\phi_{\text{upper}},\phi_{\text{lower}})_i$ on the ith piecewise cubic spline function can be determined by letting $u = 1$ or $u = 0$ find the ϕ_is using the equations of meshing $f_{3i}(X_i(u),\phi_i) = 0$ and $f_{4i}(X_i(u),\phi_{1i}) = 0$ for cases 1 and 2, respectively. Tables 4 and 5 show the working ranges $(\phi_{\text{upper}},\phi_{\text{lower}})_i$ for cases 1 and 2.

The results in Tables 4 and 5 show that the working ranges of each pair of adjacent small cutters are connective and continuous. As discussed in [9], if linear functions are chosen for the piecewise generation method, the phenomenon called "secondary generation" will occur because of tip points on fitted cutter profiles. However, since cubic spline functions with first- and second-order derivative continuity were used in this study, the phenomenon should not occur. But checking of undercutting conditions is necessary.

5. Conditions of nonundercutting

Mathematically, the problem of tooth nonundercutting involves avoiding the appearance of singular points on the generated shape Σ_2. At such points on Σ_2, tangent T does not exist, and the necessary condition for existence of singular points on Σ_2 may be represented as

Table 4
The working ranges of ϕ_i for case 1

i	$\phi_{\text{lower},i}$ (rad)	$\phi_{\text{upper},i}$ (rad)
1	−0.40608	−0.24365
2	−0.24365	−0.08121
3	−0.08121	0.08121
4	0.08121	0.24365
5	0.24365	0.40608

Table 5
The working ranges of ϕ_{1i} for case 2

i	$\phi_{\text{lower},i}$ (rad)	$\phi_{\text{upper},i}$ (rad)
1	−0.34493	−0.16809
2	−0.16809	0.00008
3	0.00008	0.17782
4	0.17782	0.33251
5	0.33251	0.63015

$$\mathbf{v}_r^{(2)} = \mathbf{v}_r^{(1)} + \mathbf{v}^{(12)} = 0, \tag{47}$$

where $\mathbf{v}_r^{(1)}$ and $\mathbf{v}_r^{(2)}$ are the velocities of points in motion along profiles Σ_1 and Σ_2 respectively, and $\mathbf{v}^{(12)}$ is the sliding velocity.

Vector equation (47) may be represented in coordinate system S_1 as follows:

$$\frac{\mathrm{d}x_i}{\mathrm{d}u}\frac{\mathrm{d}u}{\mathrm{d}t} = -v_{xi}^{(12)}, \quad \frac{\mathrm{d}y_i}{\mathrm{d}u}\frac{\mathrm{d}u}{\mathrm{d}t} = -v_{yi}^{(12)}. \tag{48}$$

Differentiating the equation of meshing

$$f_i(u, \phi_i) = 0 \tag{49}$$

gives

$$\frac{\partial f_i}{\partial u}\frac{\mathrm{d}u}{\mathrm{d}t} = -\frac{\partial f_i}{\partial \phi_i}\frac{\mathrm{d}\phi_i}{\mathrm{d}t}. \tag{50}$$

Consider system Eqs. (48) and (50) as a system of three linear equations involving one unknown. The unique solution for unknown $\mathrm{d}u/\mathrm{d}t$ exists, if the rank of the augmented matrix is equal to one, and the following second-order determinants are equal to zero:

$$\begin{vmatrix} \dfrac{\mathrm{d}x_i}{\mathrm{d}u} & -v_{xi}^{(12)} \\ \dfrac{\mathrm{d}f_i}{\mathrm{d}u} & -\dfrac{\partial f_i}{\partial \phi_i}\dfrac{\mathrm{d}\phi_i}{\mathrm{d}t} \end{vmatrix} = 0, \tag{51}$$

$$\begin{vmatrix} \dfrac{\mathrm{d}y_i}{\mathrm{d}u} & -v_{yi}^{(12)} \\ \dfrac{\mathrm{d}f_i}{\mathrm{d}u} & -\dfrac{\partial f_i}{\partial \phi_i}\dfrac{\mathrm{d}\phi_i}{\mathrm{d}t} \end{vmatrix} = 0. \tag{52}$$

Eq. (47) demonstrates that

$$\frac{\mathrm{d}x_i/\mathrm{d}u}{\mathrm{d}y_i/\mathrm{d}u} = \frac{v_{xi}^{(12)}}{v_{yi}^{(12)}}, \tag{53}$$

it can be observed that only one of the two equations, (51) or (52), yields the relationship

$$F(u, \phi_i) = 0. \tag{54}$$

Eqs. (54) and (49) determine the limiting value of u, which corresponds to the singular point on the generated shape Σ_2. To avoid undercutting shape Σ_2, it is sufficient to exclude from meshing the limiting value of u on shape Σ_1.

Our investigation shows that there is no singularity occurring on the working parts of profiles Σ_2 in cases 1 and 2 of both conventional generation and piecewise cubic-spline generation methods. However, because the second-order derivatives at every end-point of natural cubic spline are required zero, the errors in the fitted curves near the end points will be relatively larger than those at interior points when compared with the original theoretical curves. These errors sometimes result in undercutting. If one or two more data points extended from the original theoretical curves are included for fitting, but still choose the original region to generate conjugate teeth, the undercutting will disappear. Thus, the generated curves from piecewise generation will be more accurate to approach the results from conventional generation.

6. Application examples

Two engineering examples are presented in this paper to show the applications of piecewise generation method.

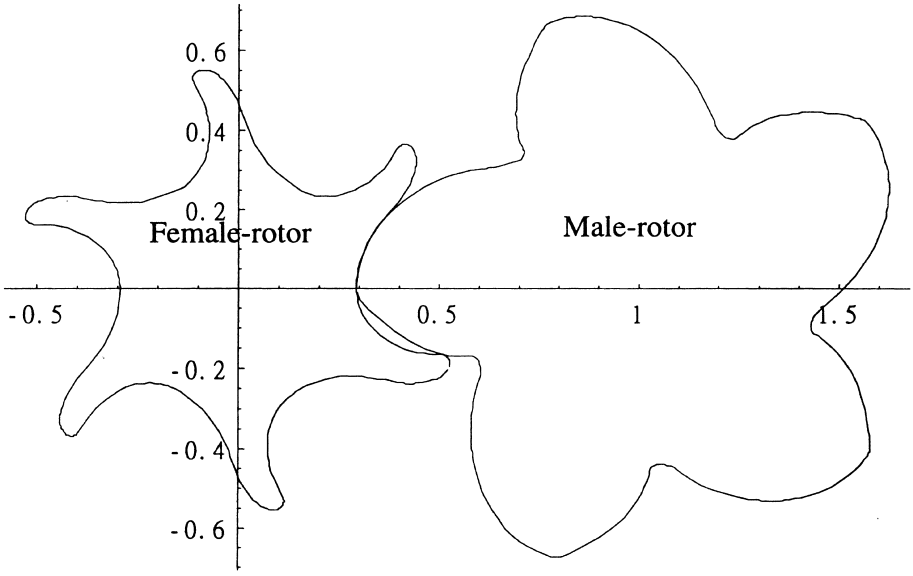

Fig. 7. Piecewise generation result for screw compressors.

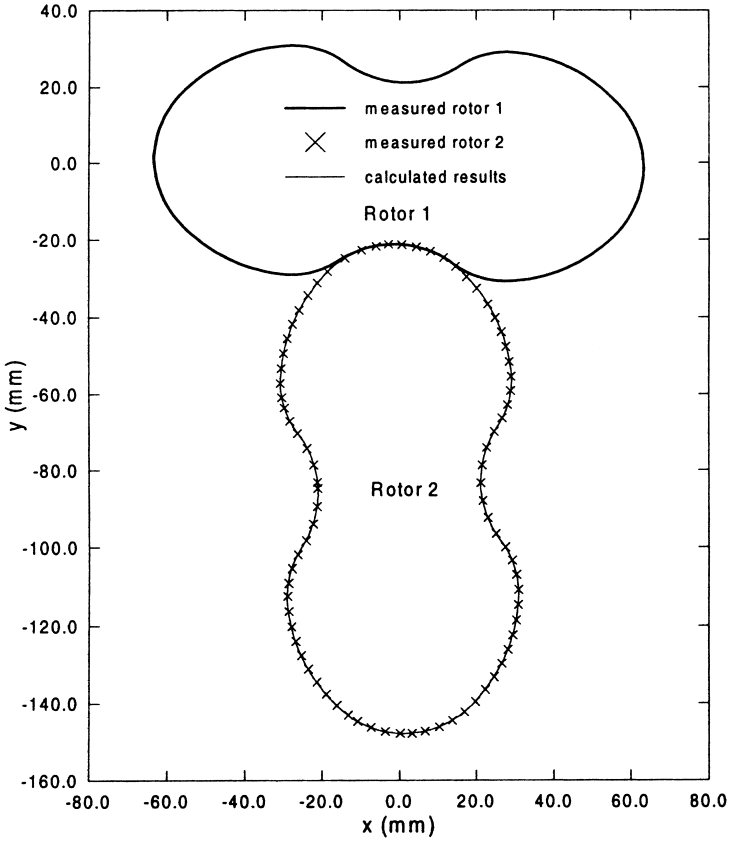

Fig. 8. Root's blower.

Table 6
Specification of ZEISS UPMC-580

3-D Accuracy	$1.7 + l/300$ (μm)
Linear resolution	0.2 (μm)
Angular resolution	0.5 arcsec

Table 7
Data point coordinates from CMM (unit: mm)

No.	x	y	No.	x	y	No.	x	y
1	0.197	−21.232	31	49.415	21.905	61	−56.712	18.050
2	3.987	−21.771	32	46.125	23.956	62	−58.876	15.348
3	7.558	−22.828	33	43.083	25.492	63	−60.782	12.084
4	10.942	−24.391	34	39.480	26.920	64	−61.937	9.275
5	14.092	−26.443	35	35.756	27.986	65	−62.724	6.463
6	17.332	−28.433	36	31.932	28.716	66	−63.241	3.413
7	20.822	−29.836	37	28.126	29.050	67	−63.376	0.733
8	24.172	−30.597	38	24.612	28.805	68	−63.013	−2.685
9	27.942	−30.841	39	21.018	27.950	69	−62.161	−6.225
10	31.802	−30.544	40	17.534	26.476	70	−60.730	−9.746
11	35.645	−29.907	41	14.469	24.639	71	−58.787	−13.019
12	39.159	−28.987	42	10.614	22.809	72	−56.360	−15.960
13	42.807	−27.65	43	6.823	21.710	73	−53.551	−18.678
14	46.318	−25.969	44	2.633	21.183	74	−50.754	−20.958
15	49.654	−23.958	45	−1.639	21.351	75	−47.471	−23.184
16	52.805	−21.646	46	−5.555	22.148	76	−44.074	−25.043
17	55.397	−19.387	47	−9.213	23.499	77	−42.594	−25.727
18	57.979	−16.572	48	−12.443	25.273	78	−40.137	−26.701
19	60.051	−13.486	49	−15.609	27.449	79	−36.434	−27.835
20	61.630	−10.134	50	−18.932	29.144	80	−32.622	−28.617
21	62.615	−6.913	51	−22.527	30.276	81	−28.811	−29.044
22	63.148	−3.836	52	−25.857	30.768	82	−25.032	−28.879
23	63.385	−1.132	53	−29.367	30.763	83	−21.704	−28.174
24	63.141	1.779	54	−33.245	30.333	84	−18.212	−26.826
25	62.459	5.182	55	−37.054	29.565	85	−15.155	−25.060
26	61.187	8.761	56	−40.764	28.438	86	−11.702	−23.257
27	59.504	11.925	57	−44.356	26.947	87	−8.108	−22.025
28	57.686	14.447	58	−47.573	25.251	88	−3.904	−21.280
29	55.284	17.037	59	−50.839	23.127	89	−0.224	−21.205
30	52.378	19.666	60	−53.906	20.717			

Example 1: Screw compressors. The rotors of a screw compressor are a kind of typical conjugate kinematic pair. The profiles of the rotors usually consist of various original curves, such as arcs, straight lines, ellipse, ..., and so on. The original curves of rotor profile used in this example are based on [10]. There are one ellipse curve and three circular arcs distributed on the rotor profiles. Totally 1355 data points are sampled from their analytical forms of the male rotor. The derivation of conjugate female-rotor profile is a very complicated work by the conventional generation method [11] because every part of the generated curves and meshing equations should be derived symbolically from the original curves, respectively. However, piecewise generation method samples the data points from male-rotor profile and the full female rotor can be determined once by using the numerical method. It simplifies the derivative procedure and makes systematic simulation on computer possible. Fig. 7 shows the results of this conjugate profiles.

Example 2: Roots blower. The data points for roots blower are measured from CMMs, and the original theoretical curves on the rotor are unknown. Conventional generation method cannot deal with this problem because the meshing equations cannot be derived from discrete points. However, piecewise generation method can do this well.

Fig. 8 shows the rotor shapes of the Roots blower. Both rotors 1 and 2 are measured from the coordinate measuring machine: ZEISS UPMC-850, its specification shown in Table 6. There are 89 data points (as listed at Table 7) in rotor 1 and 81 data points in rotor 2, respectively. Use rotor 1 as the original rotor and the conjugate results, rotor 2, by using piecewise generation can then be presented with thin lines in Fig. 8. They match the data points of rotor 2 very well, and are useful in verifying the conjugate properties.

7. Discussion

The concept of the piecewise generation method is similar to the calculus. It reduces the generation method from a large domain to a tiny domain. For any specific generation mechanism, the equation of meshing

$$\mathbf{N} \cdot \mathbf{v}^{(12)} = 0 \tag{55}$$

must be derived again symbolically every time by using conventional generation methods when the cutter profile is changed. The piecewise generation method using cubic spline functions to fit original cutters need only derive the equation of meshing once, because of the fixed form of $\mathbf{r}_i = [\, X_i(u) \quad Y_i(u) \,]$, then the analytical-form meshing equation can be determined for this generation mechanism. What we need to do is to substitute data points on the cutter into the form and then the piecewise conjugate shapes can be determined. This method makes systematic simulation possible for computer programmers. This approach can also be used to verify the results from the conventional generation method.

From an optimization standpoint, more design variables make systems more flexible in satisfying required functions. The piecewise generation method makes all data points on the cutter design variables. But they are much more than just variables in the original parametric form. If the design optimization tools are applied, this method can contribute more to conjugate-pair design.

Form a reverse-engineering standpoint, the piecewise generation method can deal with cutter data points measured using CMMs no matter what the original profile is. It is more practical and powerful than conventional generation methods used for reverse engineering.

8. Conclusions

This paper proposes a method called "piecewise generation" for generating conjugate shapes from cutters by fitting points on the cutters using cubic spline functions. Cutter data points derived from analytical forms or measured using CMMs can also be fitted with cubic spline functions. This method requires that the meshing equation be derived only once for the cubic spline functions, then the conjugate shapes can be determined for this generation mechanism. When a cutter shape is changed, the equation of meshing need not be derived again. It is quite useful and practical in conjugate-pair design verification and reverse engineering applications.

Acknowledgements

This work was supported by National Science Council, Taiwan, Republic of China, under grant number NSC86-2212-E-009-030.

Appendix A

Equation of Shape Σ_1: The normal of shape Σ_1 in case 1 is

$$\mathbf{N}_1 = \frac{d\mathbf{r}_1}{d\theta} \times \mathbf{k}_1 = \cos\psi_c \mathbf{i}_1 - \sin\psi_c \mathbf{j}_1. \tag{A.1}$$

Relative velocity $\mathbf{v}_1^{(12)}$: The velocity of the rack cutter is

$$\mathbf{v}_1^{(1)} = -\omega r \mathbf{i}_1, \tag{A.2}$$

where ω is the angular velocity of the gear, and r the radius of the pitch circle.

The linear velocity of the gear contact point is

$$\mathbf{v}_1^{(2)} = (\omega \times \mathbf{r}_1) + (\mathbf{R}_1 \times \omega), \tag{A.3}$$

where the position vector $\mathbf{R}_1$ is represented by

$$R_1 = \overline{O_1O_2} = r\phi\mathbf{i}_1 - r\mathbf{j}_1. \tag{A.4}$$

Eq. (A.3) yields

$$\begin{aligned}\mathbf{v}_1^{(2)} &= (\omega \times \mathbf{r}_1) + (\overline{O_1O_2} \times \omega)\\ &= \begin{bmatrix} \mathbf{i}_1 & \mathbf{j}_1 & \mathbf{k}_1 \\ 0 & 0 & \omega \\ \theta\sin\psi_c & \theta\cos\psi_c & 0 \end{bmatrix} + \begin{bmatrix} \mathbf{i}_1 & \mathbf{j}_1 & \mathbf{k}_1 \\ r\phi & -r & 0 \\ 0 & 0 & \omega \end{bmatrix}\\ &= \omega[(-\theta\cos\psi_c - r)i_1 + (-r\phi + \theta\sin\psi_c)j_1].\end{aligned} \tag{A.5}$$

The relative linear velocity is

$$\mathbf{v}_1^{(12)} = \mathbf{v}_1^{(1)} - \mathbf{v}_1^{(2)} = \omega[\theta\cos\psi_c\mathbf{i}_1 + (r\phi - \theta\sin\psi_c)\mathbf{j}_1]. \tag{A.6}$$

Appendix B

Equation of Shape Σ_1: In case 2, shape of Σ_1 is represented in coordinate system S_1 by

$$\mathbf{r}_1(\theta) = r_b(\sin\theta - \theta\cos\theta)\mathbf{i}_1 + r_b(\cos\theta + \theta\sin\theta)\mathbf{j}_1. \tag{B.1}$$

Its normal is

$$\mathbf{N}_1 = \frac{\mathbf{d}r_1}{\mathbf{d}\theta} \times \mathbf{k}_1 = r_b\theta\cos\theta\mathbf{i}_1 - r_b\theta\sin\theta\mathbf{j}_1. \tag{B.2}$$

Relative velocity $\mathbf{v}_1^{(12)}$: As shown in Fig. 3, gears 1 and 2 rotate about z_1 and z_2 (they are not shown in Fig. 3) with angular velocities

$$\omega^{(1)} = \omega^{(1)}\mathbf{k}_1, \tag{B.3}$$

$$\omega^{(2)} = -\omega^{(2)}\mathbf{k}_2, \tag{B.4}$$

where $\mathbf{k}_1$ and $\mathbf{k}_2$ are unit vectors of axes z_1 and z_2. The ratio of angular velocity m_{12} can be represented by

$$m_{12} = \frac{\omega^{(1)}}{\omega^{(2)}} = \frac{\phi_1}{\phi_2} = \frac{N_2}{N_1}, \tag{B.5}$$

where N_1 and N_2 are tooth numbers of pinion 1 and gear 2.

The relative linear velocity is

$$\begin{aligned}\mathbf{v}_1^{(12)} &= \mathbf{v}_1^{(1)} - \mathbf{v}_1^{(2)} = (\omega_1^{(12)} \times \mathbf{r}_1) - (\overline{O_1O_2} \times \omega_1^{(2)})\\ &= \begin{vmatrix} \mathbf{i}_1 & \mathbf{j}_1 & \mathbf{k}_1 \\ 0 & 0 & \omega_1^{(1)} + \omega_1^{(2)} \\ x_1 & y_1 & 0 \end{vmatrix} - \begin{vmatrix} \mathbf{i}_1 & \mathbf{j}_1 & \mathbf{k}_1 \\ C\sin\phi_1 & C\cos\phi_1 & 0 \\ 0 & 0 & -\omega_1^{(2)} \end{vmatrix}\\ &= -[(\omega_1^{(1)} + \omega_1^{(2)})y_1 - \omega_1^{(2)}C\cos\phi_1]\mathbf{i}_1 + [(\omega_1^{(1)} + \omega_1^{(2)})x_1 - \omega_1^{(2)}C\sin\phi_1]\mathbf{j}_1.\end{aligned} \tag{B.6}$$

References

[1] F.L. Litvin, Theory of Gearing, NASA RP-1212 (AVSCOM 88-C-035), Washington, DC, 1989.
[2] F.L Litvin, Gear Geometry and Applied Theory, Prentice Hall, New York, 1994.
[3] C.B. Tsay, Helical gears with involute shaped tooth geometry computer simulation tooth contact analysis and stress analysis, Journal of Mechanisms Transmission and Automation in Design Transactions of the ASME 110 (1988) 482–491.
[4] F. Yamaguchi, Curves and Surfaces in Computer Aided Geometric Design, Springer, Berlin, 1988.
[5] J. Hoschek, D. Lasser, Fundamentals of Computer Aided Geometric Design, A K Peters, 1993.
[6] G. Farin, Curves and Surfaces for Computer Aided Geometric Design. A Practical Guide. Academic Press, New York, 1990.
[7] H.B. Richard, C.B. John, A.B. Brian, An Introduction to Splines for use in Computer Graphics and Geometric Modeling. Morgan Kaufmann Publishers, 1987.
[8] S.H. Su, C.H. Tseng, Generating conjugate shapes using piecewise linear functions, Journal of Chinese Society of Mechanical Engineering 20 (2) (1999) 97–105.
[9] P.H. Wagner, X. Luo, K.A. Stelson, Smoothing curvature and torsion with spring splines, Computer-Aided Design 27 (8) (1995) 615–626.
[10] H.T. Lee, Screw-Rotor Machine With an Ellipse As a Part of Its Male Rotor, US Patent 4, 890,992 1990.
[11] S.H. Su, C.H. Tseng, Synthesis Method for Cross-Sectional Rotor Profiles of Screw Compressors, IASTED International Conference on Applied Modelling and Simulation, Hawaii, 1998, pp. 147–151.